Journal Pre-proof

Nanocomposite starch films: Cytotoxicity studies and their application as cheese packaging

F. Ortega, J. Minnaard, V.B. Arce, M.A. García

PII: S2212-4292(23)00213-4

DOI: https://doi.org/10.1016/j.fbio.2023.102562

Reference: FBIO 102562

To appear in: *Food Bioscience*

Received Date: 9 January 2023

Revised Date: 7 March 2023

Accepted Date: 11 March 2023

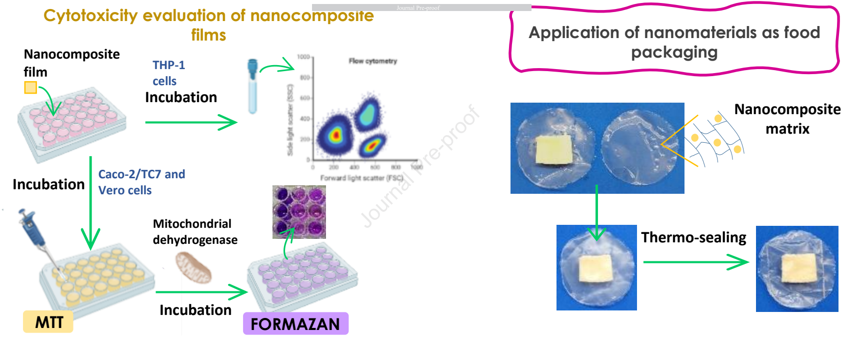
Cytotoxicity evaluation of nanocomposite films
Nanocomposite film
THP-1 cells
Incubation
Flow cytometry
Side light scatter (SSC)
Forward light scatter (FSC)
Incubation
Caco-2/TC7 and Vero cells
Mitochondrial dehydrogenase
MTT
Incubation
FORMAZAN
Application of nanomaterials as food packaging
Nanocomposite matrix
Thermo-sealing

Nanocomposite starch films: cytotoxicity studies and their application as cheese packaging

F. Ortega[1,2], J. Minnaard[1,2], V.B. Arce[3,2], M.A. García[1,2]

[1]CIDCA- UNLP- CONICET- CICPBA, 47 y 116 (1900), La Plata, Argentina

[2]Facultad de Ciencias. Exactas, UNLP, 47 y 115 (1900.), La Plata, Argentina

[3]CIOP-UNLP-CICPBA, Camino Centenario e/505 y 508, (1897) Gonnet, Argentina

*** Corresponding author:** Maria Alejandra Garcia

e-mail: (magarcia@quimica.unlp.edu.ar) tel/fax: +54-221-4254853/+54-221-4249287

address: 47 & 116 Street (1900), La Plata, Argentina

Abstract

This work focuses on the development of starch-based nanocomposite films containing AgNPs obtained by different green synthesis techniques, the characterization of their relevant properties, the study of their cytotoxicity and their application as food packaging on cheese.

AgNPs were obtained by different green synthesis techniques: AgNP *in situ* and AgNP L. The incorporation of AgNP L improved the barrier properties of nanocomposite films, since water vapor permeability decreased ($0.63 \pm 0.07 \times 10^{-10}$ g / m s Pa) compared to films containing AgNPs *in situ* ($1.9 \pm 0.1 \times 10^{-10}$ g/ m s Pa), while the UV-vis barrier capacity was higher (371.5 ± 15.6 and 314.1 ± 14.7, respectively). Films with AgNPs synthesized *in situ* were less cytotoxic for the Caco-2/TC7 line (90% viability) in comparison with films containing AgNPs synthesized with lemon juice (AgNP L). Vero cells were susceptible to adhesion problems on both control and nanocomposite films. Likewise, the differences observed between monocytes and macrophage THP-1 cells may be associated with the expression of different markers. Then, active packages were developed by thermo-sealing the films. The nanocomposite samples were able to extend the shelf life of cheese by 7 days, but the CL and AgNP L films were more effective, probably due to the synergistic effect of the active compounds present in the lemon juice and the low pH of the film-forming suspension. Finally, production costs and the current legislative framework for this type of material were revised.

Keywords: silver nanoparticles, nanocomposite materials, cytotoxicity evaluation, active packages, thermo-sealing, cheese.

Abbreviations

Citric acid (CA)

Control DMEM (CM)

Control AgNP *in situ* (CS)

Control AgNP L (CL)

Dulbecco's Modified Eagle Medium (DMEM)

3-(4,5-dimethylthiazol-2-yl)-2,5 diphenyl tetrazolium (MTT)

Elastic modulus (EM)

Elongation at break (EB)

Fetal bovine serum (FBS)

Phosphate buffered saline (PBS)

Tensile strength (TS)

Silver nanoparticles (AgNP)

Silver nanoparticles synthesized *in situ* (AgNP *in situ*)

Silver nanoparticles synthesized using lemon juice (AgNP L)

Water vapor permeability (WVP)

1. Introducción

Nanotechnology has expanded rapidly in the last 5 years, with about 17,000 publications related to the green synthesis and characterization of nanoparticles (NPs) and the production of environmentally friendly nanocomposite materials, according to the Scopus database as of November 2022.

Biopolymers are a suitable medium for the synthesis and stabilization of AgNPs, as they allow a good dispersion of the nanoparticles within the matrix, which ultimately influences the stability and homogeneity of the film (Mathew et al., 2019; Qin et al., 2019; Rafique et al., 2017). According to Kraśniewska et al. (2020), the techniques for obtaining nanocomposite films depend on how the nanoparticles are synthesized and can be divided into two methods: *in situ*, where the polymeric matrix is used as a reaction medium for the formation of AgNPs and acts as a stabilizing agent for them (Ortega et al., 2017, 2019); and *ex situ*, where the polymeric matrix is mainly used as a dispersion and stabilization medium for separately synthesized nanoparticles (Ortega et al., 2021).

In reference to nanocomposite materials with antimicrobial activity, factors such as size, shape, and Ag concentration, in addition to the NP-polymer interaction, must be considered. In this sense, good antimicrobial activity against Gram-positive and Gram-negative bacteria was observed in the obtained nanocomposite materials (Ortega et al., 2017; 2019). For this reason, NPs are incorporated into food contact materials because they can improve and extend the food shelf-life, but they must be safe, environmentally friendly, and cost-effective to obtain (Rizzotto et al., 2022; Vanlalveni et al., 2021).

In view of the potential use of these materials, toxicological analysis is crucial, as there is a possibility that nanoparticles may migrate into food and be ingested by consumers of the product. In this regard, studies, and regulations on the migration of AgNPs in food simulants are not well established. In July 2021, the EFSA Panel on Food Contact Materials, Enzymes and Processing Aids (CEP) (Lambré et al., 2021) assessed the safety of additive AgNPs intended for use in plastics. They concluded that AgNPs with a mean diameter of approximately 15 nm do not pose a safety concern to the consumer when used as an additive up to 0.025% w/w in synthetic polymers that do not swell in contact with aqueous foods and food simulants. On the other hand, European Union legislation (Commission Regulation, 2011. (EU) No 10/2011 on Plastic Materials and Articles Intended to Come into Contact with Food) has set general migration limits for food contact material additives at 10 mg/dm^2 or 60 mg/kg of simulant. Several authors have investigated the migration of AgNPs from different polymeric materials (Kim et al., 2019; Polat et al., 2018; Störmer et al., 2017). In a previous work (Ortega et al., 2022) the release of AgNP *in situ* and AgNP L included in starch-based nanocomposite films to food simulants (water, acetic acid, and ethanol) was studied. The released Ag (mg Ag/kg simulant) was higher for films with AgNPs *in situ*. Regardless of the maximum values obtained, these were lower than the limit established by EU legislation and the national standard, which establishes global migration limits at 8 mg/dm^2 or 50 mg/kg of food or simulant (MERCOSUR, Resolution MERCOSUR N_ 36/92 and Res. Conj. 140 and 526/01). On the other hand, the bio-disintegration of the developed nanocomposite materials was demonstrated over a period of 90 days under composting conditions. The eco-toxicity test allowed inferring that the bio-disintegration of the studied films did not contribute substances with phytotoxic activity to the compost under the evaluated conditions, allowing the germination of fast-growing species that are indicators of phytotoxicity (Ortega et al., 2022).

When considering the application of these nanocomposite materials as food packaging, it is necessary to evaluate the cytotoxicity of AgNPs. There are few studies that go further by evaluating the cytotoxicity of the materials developed and why the cell lines tested were chosen. For this purpose, assays are used on different cell lines related to the intestinal epithelium, such as Caco-2 and FHC, fibroblasts, such as Vero, Huh7 liver cells, THP-1 monocytic cells, among others (Abdallah et al., 2020; Böhmert & Niemann, 2014; Hasanin, et al., 2021; Yu et al., 2019). Although there are numerous works reporting on the development of nanocomposite materials, including some that propose applications in the food area (Leites Luchese et al., 2021; Mangaraj et al., 2019; Mathew et al., 2019; Noshirvani et al., 2017; Zhai et al., 2018), there are few investigations reporting on the study of the cytotoxicity of materials containing AgNPs, which is crucial for progress in this regard. Likewise, to scale up the production of these materials, it is important to estimate, at least, the costs of the necessary inputs and to relieve the regulatory aspects that these materials must satisfy.

Cheese has been proposed by several authors as a model system to evaluate the performance of different materials used as packaging since it is a biologically and biochemically unstable food, making its conservation a challenge (Cerqueira et al., 2010; Jafarzadeh et al., 2021; López et al., 2013; Lucera et al., 2014). This dairy product is exposed to different microbial and chemical deteriorations during manufacturing, processing, and storage (Ferrão et al., 2016). Cheese surface is susceptible to contamination by bacteria and fungi due to its acidity conditions and relative high-water activity (Proulx et al., 2017). One of the most desirable approaches to increase cheese shelf-life is using the proper packaging, which leads to reducing biochemical, microbiological, physical and chemical deterioration, as well as enhancing the handling and marketing of cheese (Khoshgozaran et al., 2012). In this sense, the use of nanocomposite films as cheese packaging has been scarcely studied (Jafarzadeh et al., 2021).

Thus, the aims of this work were to develop nanocomposite starch-based films containing AgNPs obtained by different green synthesis techniques, to characterize their relevant properties, to study their cytotoxicity and to evaluate their applications as food packaging on cheese.

2. Materials and methods

2.1. Materials

Native corn starch with 25% amylose was provided by Unilever (Buenos Aires, Argentine) and glycerol (Anedra, Buenos Aires, Argentine) was used as a plasticizer. For nanocomposite films containing AgNPs *in situ*, silver nitrate ($AgNO_3$) and maltose (reducing agent) were purchased from Biopack (Buenos Aires, Argentine) and for the samples with AgNP L, lemons (*Citrus limon*) used were grown in La Plata city, Argentine (34°56’26”S 57°59’44” W). The rest of the reagents used were of analytical grade.

2.2. Obtention of nanocomposite starch films

Nanocomposite starch films including AgNPs were obtained by *casting* method according to Ortega et al. (2017-2021). Briefly, for the materials with AgNPs *in situ* a filmogenic suspension with native corn starch (3% w/v) was gelatinized, then 10 ml of $AgNO_3$ $6.5x10^{-4}$ M was added such that the final concentration of Ag in the films was 143 ppm, and 20 ml of maltose ($1.3x10^{-3}$ M) solutions were incorporated as reducing agent. The system was kept under stirring at 90 °C for 20 min.

To obtain films with AgNP L the volume of 1920 µl of AgNP L was mixed with 100 ml of 3% w/v corn starch suspension and gelatinized at 90 °C for 20 min as specified in Ortega et al. (2021).

In both cases, after gelatinization, the nanocomposite filmogenic suspensions were cooled at 50 °C and 30% w/w glycerol (Anedra, Buenos Aires, Argentine) was added as a plasticizer and then dried in an air forced convection oven GRX-9203A (Bluepard Instruments Co., Shanghai, China) (50 °C for 5 h).

The CS and CL films correspond to the starch polymer matrix without nanoparticles and were obtained according to Ortega et al. (2017, 2021).

2.3. Silver nanoparticles characterization

To characterize the AgNPs' suspension 3 ml were taken and analyzed by UV-vis absorption spectroscopy according to (Ortega et al., 2017, 2021) using a T90+ UV/vis Spectrometer (PG Instruments Limited, Leicestershire, UK). After the nanoparticles were obtained the size and morphology were analyzed by transmission electron microscopy (TEM) JEOL-JEM 1200EXII, (Jeol, Tokyo, Japan) equipped with an Erlangshen ES1000W, Model 785 (Gatan Inc., Pleasanton, California, USA) camera and the images were processed using the ImageJ Software™ (Schneider, Rasband, & Eliceiri, 2012).

Zeta potential (**ζ**) was measured in a SZ-100 Nano particle analyzer (Horiba Scientific, Kyoto, Japan) applying a voltage 3.3 V at 25 °C. Determinations were performed at least in duplicate.

2.4. Characterization and films' properties

2.4.1. Microstructural characterization of nanocomposite films

Infrared spectroscopy by Fourier transform with attenuated total reflectance (ATR-FTIR) was determined as mentioned in Ortega et al. (2022) using a Nicolet-iS10 FTIR spectrometer (Thermo Scientific, Waltham, MA, USA) with attenuated total reflection.

To evaluate the films' crystallinity X-ray diffraction (XRD) analyses were carried out using a X´Pert Pro PAnalytical Model PW 3040/60 (Malvern Panalytical, Almelo, Netherlands) diffractometer equipped with a Cu K_α radiation (λ=1,543 nm) and a detector operating at 40 kV and a current of 40 mA. The diffraction patterns were obtained in the range of 2θ = 3° to 60°. The crystallinity (%) was calculated according to Versino and García (2019).

The morphology of obtained films were examined by scanning electron microscopy using a FEI QUANTA 200 SEM (FEI Company, Hillsboro, OR, USA) with an Apolo 40 electron detector and acceleration voltage of 10 kV according to Ortega et al. (2019).

2.4.2. Films' optical properties

The surface color of the films was measured using a Konica Minolta CR Series 300 (Konica Minolta, Tokyo, Japan). Samples were placed on a white standard plate (L* = 97.44, a* = −0.06 and b* = 1.78) and at least five measurements were taken. Luminosity (L*) and chromaticity parameters (a* and b*) were registered using the CIELab color scale.

The film transparency was calculated as the absorbance value at 600 nm divided by film thickness and was expressed as A600/mm, and the UV–vis barrier capacity as the area under the absorption curve between 200 and 700 nm as described in a previous work (Ortega et al., 2019).

Film thickness was measured using a digital ultrasonic thickness gauge meter CM-8822 (REED Instruments, NY, USA), on a non-ferrous surface for non-conductive materials. The mean value of fifteen measurements on different positions was reported.

2.4.3. Films' solubility and moisture content

Solubility (%) and moisture content (%) were calculated as described (Ortega et al., 2017).

Briefly, for the solubility's determination at 25 °C, the film samples (2 × 2 cm^2) were weighed and then stirred at 200 rpm for 1 hour in beakers containing 80 ml of ultrapure water. Finally, the samples were recovered by filtration and dried at 105 °C to a constant weight.

The moisture content was determined by measuring the weight loss of the films after drying in an oven at 105 °C to constant weight.

The reported results corresponded to the mean of at least two replicate assays.

2.4.4. Films' water vapor permeability

WVP tests were conducted using the ASTM method E96 with several modifications according to López et al. (2008). Assays were performed at least in triplicate and results were expressed in (g / m s Pa).

2.4.5. Films' mechanical properties and heat-sealing capacity

Mechanical properties of the films were analyzed using a TA.XT2i-Stable Micro Systems (Godalming, UK) texturometer with an A/TG tension grip system. Ten probes (0.6 × 7 cm^2) were tested at a strain rate of 5 mm/s in the pre-test and 1 mm/s in the assay. According to the ASTM D882-91 method, EM (MPa), TS (MPa) and EB (%) were calculated as was previously described (Ortega et al., 2017).

The heat-sealing capacity was studied using an impulse-wire thermosealer (HermePlas, Buenos Aires, Argentine) on film samples of 9 cm diameter. Heat-sealing resistance was evaluated using the above mentioned texturometer (Stable Micro Systems) and A/TG tension grips onto nine probes (0.6 ×7 cm^2). Mechanical patterns were registered, and the maximum tensile resistance (MPa) was calculated according to ASTM standard method F 88-00 (2001).

2.5. Cytotoxicity evaluation of nanocomposite films

The cytotoxicity of nanocomposite films was determined by evaluating the cell viability through mitochondrial dehydrogenase activity test in Caco-2/TC7 and Vero culture cells, and propidium iodide stain on the monocytic cell line THP-1.

2.5.1 Caco-2/TC7 and Vero cells

Caco-2/TC7 cells were grown in DMEM with 25 mM glucose (GIBCO Life Technologies, Grand Island, USA), 15% inactivated (30 min, 58 ºC) FBS (Internegocios S.A., Buenos Aires, Argentine), 1% not-essential amino acids (GIBCO Life Technologies, Grand Island, USA) and 12 UI/ml and 12 μg/ml of penicillin and streptomycin (Life Technologies, Cergy, France), respectively. Cells were inoculated into 24- or 48-well plates (JetBiofilm, China) at a rate of $2.5x10^5$ cells/ml and incubated at 37 ºC in a 5% CO_2 atmosphere for 7 days.

Vero cells were grown using the same medium as described for Caco-2/TC7 but supplemented with 10% FBS (Internegocios S.A) and incubated under the same conditions for 48 h. Inoculated cells were used at a rate of 2.5 x 10^5 cells/ml in plates (JetBiofilm) with 24- or 48- wells.

The effects of AgNPs on Caco-2/TC7 and Vero cells were evaluated by conversion of MTT to an insoluble purple formazan by mitochondrial dehydrogenases according to Minnaard et al. (2001) with some modifications. Film samples (5 × 5 mm^2) were sterilized under UV light for 5 min on both sides, while the cells into the culture plates were washed two times with phosphate buffered saline (PBS) and 200 μl of DMEM (GIBCO Life Technologies) was added per well. Finally, the sterilized samples were placed on the culture cells and incubated at 37 ºC in 5% CO_2 atmosphere for 1 and 24 h for both Caco-2/TC7 and Vero cells. Then the samples were removed, the cells were washed three times with PBS and 250 μl of MTT (Sigma Aldrich Co., St. Louis, MO, USA, 0.5 mg/ml) per well were added, incubating 2 h at

37 ºC. MTT was then removed, and purple formazan crystals were solubilized from the cells using 200 µl of DMSO (Biopack, Buenos Aires, Argentine). Absorbance was measured at 550 nm using a Synergy HT fluorescence microplate reader (Biotek Instruments, Winooski, VT, USA). Cell viability (%) was calculated as:

$$Cell\ viability\ (\%) = \frac{Am}{Ac} \times 100$$

where *Am* is the samples' absorbance and *Ac* is the absorbance of control cells. The informed values corresponded to the mean of at least three determinations.

CM and controls polymeric matrix (CS and CL see section 2.2) were also analyzed.

2.5.2 THP-1 cells

The THP-1 cells were grown in DMEM (GIBCO Life Technologies) medium supplemented with 10% FBS (Internegocios S.A) according to Assad et al. (2021) and 0.5 ml (per well) of $1.3x10^6$ cell/ml suspension were placed in a 24- well plate (JetBiofilm). Afterwards, the films' samples were placed on the culture cells, as aforementioned and incubated for 1 or 24 h at 37 ºC in a 5% CO_2 atmosphere. After that, the samples were removed, and cells were washed three times with cold PBS. Finally, the cells were resuspended in 200 µl PBS for a flow cytometry analysis.

To differentiate the THP-1 cells to a macrophage-like phenotype the culture was treated with Phorbol-12-myristate-13-acetate (PMA, 200 nmol L^{-1} final concentration) (Sigma Aldrich) (Assad et al., 2021). The cells in a 24-well plate were washed twice with cold PBS and the films' samples were added with DMEM (GIBCO Life Technologies) 500 µl and then treated as mentioned above for the undifferentiated THP-1 cells.

To determine the cell viability, propidium iodide (PI) (Sigma Aldrich) (1 µg/ml) was added to each tube immediately before flow cytometry analysis with a blue-green excitation light (488 nm Argon-ion laser) in a FACSCalibur™ (BD Bioscience, Franklin Lakes, NJ, USA) equipped with a CellQuest™ software. Gating of cells was performed in *SSC* vs. *FSC* scatter plot, and these were analyzed according to the red fluorescence (channel FL2+). The analysis of the results was carried out using the FlowJo™ V10.4 program and results were expressed as percentage of FL2+ cells.

2.6. Application of the nanomaterials as food packaging on cheese

To evaluate the effectiveness of the nanomaterials as active food packaging, the films were used to package a dairy product. A commercial soft cheese from whole cows' milk, with a fat content of 45%–60%, and moisture content of 46%–55% (data provided by the supplier) was used. According to Ortega et al. (2017) with some modifications, regular portions of soft cheese (10 g) were packed in thermosealed bags obtained from nanocomposite starch films. Portions of soft cheese deposited on Petri dishes were used as controls. All samples were placed in PD 141 (CRYOVAC®, Elmwood Park, NJ, USA) synthetic bags, a 75 μm thick low-density polyethylene, and stored at 4 °C.

2.6.1 Microbiological quality of cheese packaged with nanocomposite films

Lactic acid bacteria, yeast and molds were counted at initial time and after 7, 14, and 21 days of refrigerated storage. For this, cheese samples (10 g) were homogenized in a Stomacher Seward Model 400 (Seward Laboratory Systems Inc., Worthing, United Kingdom) at 230 rpm for at least 1 min with 90 ml of 0.1% p/v sterile peptone water. To reduce the sampling error, duplicates of the homogenate were made. Dilutions of the homogenate were used to inoculate MRS agar plates (de Man, Rogosa and Sharpe, BIOKAR; Biokar Diagnostics, Beauvais, France) or YGC agar plates (Yeast extract, glucose, chloramphenicol, Merck, Darmstadt, Germany) and they were incubated for 24 h at 37 °C or 5 days at 25 °C, respectively. Viable microorganism counts were determined by counting the number of colonies formed, expressing the results as CFU/g of cheese. All tests were conducted in triplicate.

2.7. Statistical analysis

All experiments were performed at least in duplicates, with individually prepared and casted films as replicated experimental units as described previously in each determination. Systat software (SYSTAT, Inc., Evanston, IL, USA) version 10.0 and InfoStat version 2020 (InfoStat Group, FCA, National University of Córdoba, Argentine) were used for multifactor analysis of variance as well as linear and nonlinear regressions. Differences in the films' properties were determined by Fisher's least significant difference (LSD) mean discrimination test, using a significance level of α= 0.05. Likewise, a Principal Component Analysis (PCA) was carried out to analyze the interdependence between the characteristics of the NPs obtained by different synthesis techniques and the relevant properties of the derived nanocomposite materials. Biplot graphs and the cophenetic correlation coefficient's values were reported, the latter being indicative of the quality of the grouping of the variables according to the components. The aforementioned software was used for this purpose.

3. Results and discussion

3.1. Silver nanoparticles obtained by different green synthesis

The silver nanoparticles were synthesized through the chemical reduction of Ag^{+} by maltose in AgNPs *in situ*, and by the active compounds present in the lemon juice in the AgNP L. The obtention was followed using UV-vis spectroscopy, since it is a simple and widely used analytical technique to monitor the formation of nanoparticles. The metal NPs exhibit different colors depending on their size and morphology, due to the excitation of the surface plasmon resonance (SPR) and usually, spherical nanoparticles exhibit a single SPR band in the absorption spectra. (Sun & Xia, 2003; Wu et al., 2016). Figure 1 shows the characteristic SPR band for the AgNPs with an absorbance maximum at 431 nm for AgNPs *in situ* and 470 nm for AgNP L (Ortega et al., 2017, 2019, 2021). The SPR band shift would be related to the different sizes of the silver nanoparticles, 14.2 ± 4.4 and 5.5 ± 0.8 nm for AgNPs *in situ* and AgNP L, respectively. Rather et al. (2018), observed a similar behavior when studying the effect of reducing sugars in the synthesis of Ag and Cu nanoparticles. These authors suggest that, depending on the structure and number of monomeric units in the carbohydrates, they would bind differently with the NPs during the capping step, resulting in different degrees of stabilization and size variation. In the case of AgNP L, the anomeric carbon in both glucose and fructose, supplied by lemon juice, allows them to act as good reducing agents, obtaining smaller nanoparticles. According to Selvakumar et al. (2016), the amplitude observed in the plasmon of AgNP L can be attributed to the different compounds present in the lemon juice such as, CA, ascorbic acid, vitamins, among others.

When analyzing the nanocomposite suspension by TEM, it was found that in general, the AgNPs had a spherical morphology with a good dispersion in the suspension (Fig. 1). Using the ImageJ software, the average diameter of the silver nanoparticles was determined, being significantly ($p<0.05$) smaller than the NPs synthesized with lemon juice as a reducing and stabilizer agent (Table inserted in Fig. 1). This difference may be explained considering that, at the same synthesis temperature (90 ºC) the compounds in the lemon juice (mainly ascorbic and citric acid, reducing sugars and polyphenols) are consumed more quickly leading to the formation of smaller nanoparticles.

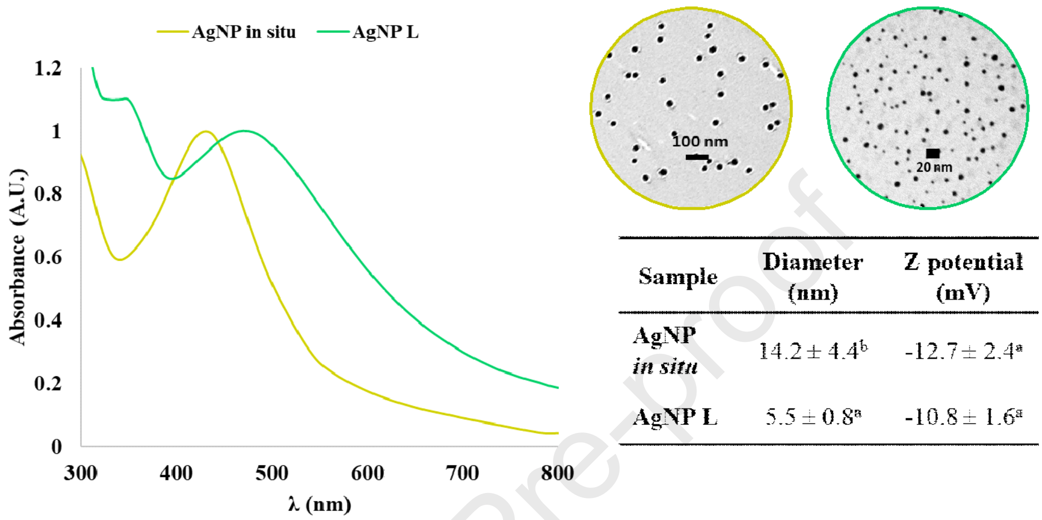

Sample	Diameter (nm)	Z potential (mV)
AgNP *in situ*	14.2 ± 4.4[b]	-12.7 ± 2.4[a]
AgNP L	5.5 ± 0.8[a]	-10.8 ± 1.6[a]

Figure 1: Effect of silver nanoparticles synthesis method on: surface plasmon resonance and morphological and stability characteristics.

The stability of the nanocomposite suspensions was evaluated through ζ potential measurements, and the obtained results were -12.7 ± 2.4 and -10.8 ± 1.6 mV for AgNPs *in situ* and AgNP L, respectively (Table inserted in Fig. 1). In agreement with Singh et al. (2014) during the metal reduction by the reducing sugars, the latter is oxidized to their corresponding acids compensating the Van der Waals forces between the particles due to the negative charge formed around the nanoparticles. In addition, in the case of AgNP L, the negative values are indicative that reducing sugars, ascorbic acid, and polyphenols, are responsible for the reduction and stabilization of NPs (Ortega et al., 2019, 2021). Other authors (Kahrilas et al., 2014; Kaviya et al., 2011; Selvakumar et al., 2016) obtained stable and spherical AgNPs with a small degree of agglomeration using citric peel and juice extracts, respectively. Although the chemical reduction of a silver salt with organic reagents is the most widely used and profitable method for a large-scale synthesis of NPs, the implementation of plant extracts is economically convenient since present a dual function of formation and stabilization of nanoparticles in aqueous medium and, they do not require high temperatures and long reaction times reducing the energy consumption. Several works have reported the obtention of other metal nanoparticles using plant extracts (Hashem et al., 2018; Jayachandran et al., 2021; Sarwar et al., 2021).

3.2. Characterization of nanocomposite starch films

By the casting method it was possible to obtain homogeneous nanocomposite starch films. In both cases, the AgNPs *in situ* and AgNP L did not affect the filmogenic capacity of starch suspensions and the materials were easily peeled-off from the plates without breaking. Furthermore, the samples with AgNP L took a slightly orange hue and the thickness did not present significant ($p>0.05$) differences as shown in Table 1.

Regarding optical properties the luminosity (L*) increased significantly ($p<0.01$) for the samples containing AgNPs *in situ* due to in films with AgNP L the presence of other components in the lemon extract may be influencing this parameter (Table 1). On the other hand, the flavonoids and phenolic compounds of the lemon juice could significantly improve ($p<0.01$) the UV-barrier capacity of the AgNP L films (Ortega et al., 2021).

Table 1 shows that the AgNP L films exhibit a significantly ($p<0.05$) lower water vapor permeability than samples with AgNPs *in situ*, because of the action of the CA (present in the lemon juice) as crosslinker. The effect of nanoparticles addition on the corn starch films' WVP was previously discussed (Ortega et al., 2017, 2021).

Table 1: Summary of relevant properties of nanocomposite starch-based films.

Film property	Nanocomposite starch based films	
	AgNP *in situ*	AgNP L
Thickness (μm)	102.0 ± 6.7[a]	102.7 ± 3.9[a]
Luminosity (L*)	94.7 ± 0.7[b]	88.1 ± 0.5[a]
UV-vis barrier capacity (200 - 700 nm)	314.1 ± 14.7[a]	371.5 ± 15.6[b]
Transparency (mm^{-1})	4.5 ± 0.3[a]	7.9 ± 0.6[b]
Solubility at 25 °C (%)	34.2 ± 0.5[a]	40.9 ± 0.6[b]
WVP × 10^{-10} (g/ m s Pa)	1.9 ± 0.1[b]	0.63 ± 0.07[a]
Tensile strength (MPa)	5.8 ± 0.3[b]	4.0 ± 0.6[a]
Elastic Modulus (MPa)	15.2 ± 0.3[a]	14.2 ± 1.8[a]
Elongation at break (%)	32.5 ± 0.7[a]	40.0 ± 5.6[b]
Heat sealing capacity (maximum tensile resistance, MPa)	1.30 ± 0.17[a]	1.8 ± 0.4[a]
Antimicrobial capacity against[1,2]	*Salmonella spp., E. Coli, S. aureus, Penicillium spp.*	*Salmonella spp., E. Coli, P. aeruginosa, S. aureus*
Ag diffusion coefficient in water (cm^2/s)[3]	3.41 ×10^{-9}	5.61 ×10^{-10}
Ag diffusion coefficient in 3% v/v acetic acid (cm^2/s)[3]	1.99 ×10^{-9}	1.53 ×10^{-9}
Ag diffusion coefficient in 15% v/v ethanol (cm^2/s)[3]	3.68 ×10^{-9}	3.72 ×10^{-9}
Bio-disintegration in soil after 90 days (%)[3]	56.3	49.4
Compost ecotoxicity[3]	No present	No present

Means ± SD values are presented. Different letters within the same column indicate significant differences ($p<0.05$). [1] Ortega et al. (2017), [2] Ortega et al. (2021), [3] Ortega et al. (2022).

The X-ray diffractograms and the crystallinity degree (CD, %) of the control and nanocomposite films are shown in Figure 2a. The control starch films presented a semi-crystalline pattern with diffraction peaks around 2θ=17.8; 20 and 22.7º, with small deviation in accordance with the results obtained by López (2011). In addition, the inclusion of AgNPs *in situ* did not significantly modify the crystalline morphology of the starch matrix. The characteristic diffraction peaks mentioned by Mohan et al. (2016) for crystalline planes of the face-centered cubic (fcc) of Ag (2θ= 37.6; 43.8; 63.85 and 77.15º, corresponding to the (111), (200) and (311) planes, respectively were not observed, because the signals of the starch matrix are overlapped to the Ag signal at low concentration in the films. For the samples containing AgNP L (3.74 wt% CA for this concentration of 71.5 ppm) no new peaks appear in the diffractogram, but a slight decrease in intensity is observed at 20 and 22º with respect to the control film and that with AgNP *in situ*. Shi et al. (2008) studied the effect of different concentrations of CA (5 - 30 wt%) on the structural properties of PVA/starch films and stressed that both the plasticizing and crosslinking effects of CA lead to a decrease in crystallinity. It has been suggested that the incorporation of CA affects the crystallinity of starch-based films by generating crosslinks in the matrix, stiffening the structure, and modifying the alignment of the polymeric chains, although some of the amorphous zones of the starch may have been better oriented after crosslinking. (Reddy & Yang, 2010; Shi et al., 2008). The inclusion of AgNP L to the starch matrix partially reverts the action of CA, and this supports what was discussed in Ortega et al. (2021) where it is pointed out that the incorporation of up to 5% CA induces the crosslinking of the polymeric chains and that there is a reinforcement in the materials by incorporation of 71.5 ppm of AgNP L. As well as for the AgNPs *in situ*, it was not possible to visualize the peaks corresponding to Ag due to the low concentration of AgNP L incorporated to the films.

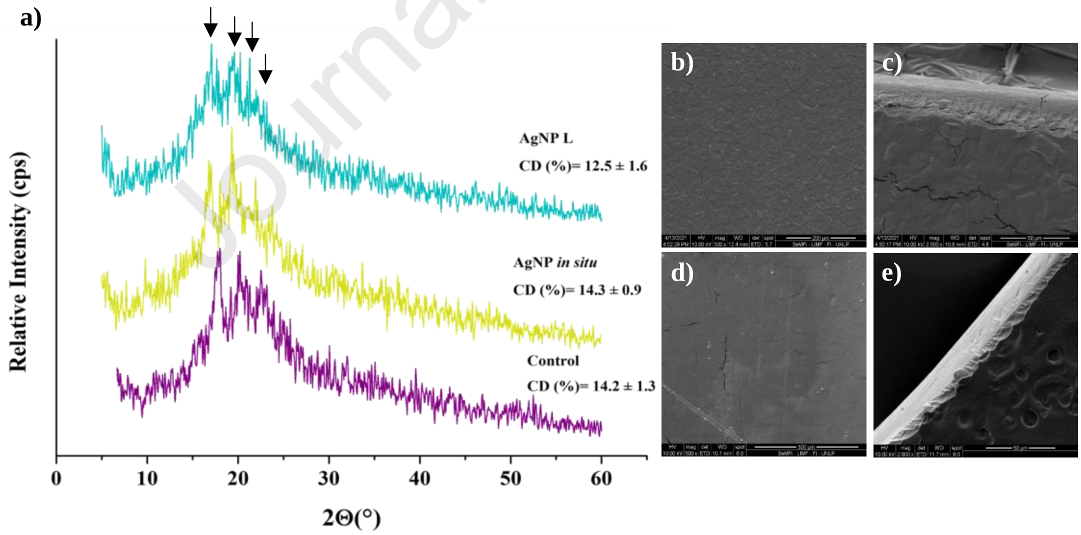

Figure 2: a) Diffractograms and crystallinity degree (CD, %) of control and nanocomposite films and SEM micrographs of starch based films containing AgNP L (b, c) and AgNP *in situ* (d,e).

Regarding the microstructural characterization of the nanocomposite systems, SEM micrographs (Fig. 2. b-e) showed that the AgNPs were integrated in the polymeric matrix and ATR-FTIR analysis discussed in Ortega et al. (2022) confirmed the participation of the OH groups of the starch in the stabilization of the synthesized AgNPs.

The principal components analysis (PCA) allowed the integration of the AgNPs' characteristics obtained by different green synthesis techniques with the relevant properties of the nanocomposite materials that will condition their subsequent application, also integrating the results of nanoparticles migration and biodegradation (Fig. 3). The total variance could be explained by two principal components (CP1= 55.4% and CP2= 44.6%). The cophenetic correlation was 1.0 indicating that the association of the variables would be appropriate. CP1 differentiated between control and nanocomposite samples, while CP2 discriminated according to the CA content and other compounds provided by the lemon juice. Films with AgNP *in situ* were placed next to the TS, particle diameter and amount of Ag that migrated to the simulants water and 3% v/v acetic acid, respectively, after 7 days (Ag/water and Ag/AA). These results agree with previously reported (Ortega et al., 2017, 2019, 2022) since, AgNPs *in situ* presented a higher diameter, reinforced the starch matrix, and migrated more to the simulant media compared to AgNP L. This may be related with the Ag concentrations incorporated in each case. The AgNP L films were situated near the material EB, EM, and thickness, in agreement with Table 1. It should be noted that in the biplot graph, the bio-disintegration (BD) and the FTIR peaks' absorbance ratio 1022/995 (associated with the contribution of the amorphous zones) were located in the same quadrant and in opposition to the EM, since the reinforcement of the matrix is evidenced by higher EM values and consequently a more rigid structure is less accessible to attack by soil microflora, requiring more time for biodegradation, which is evidenced in Table 1, since the % biodegradation at 90 days for AgNPL films is significantly lower.

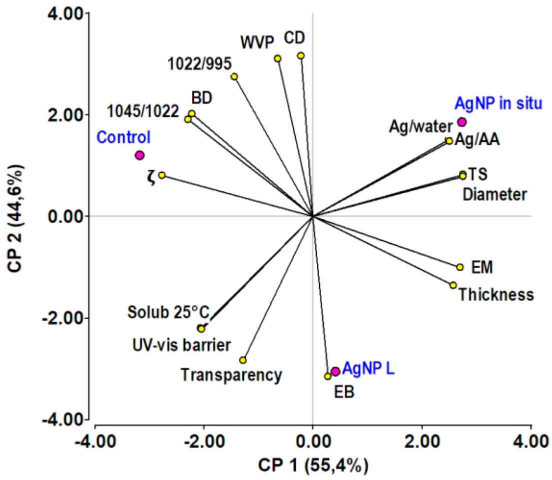

Figure 3: Biplot graph resulting from the PCA of the main film properties of nanocomposite films and the characteristics of the nanocomposite filmogenic suspensions (yellow dots) containing AgNP *in situ* and AgNP L, (red dots). The properties analyzed were: optical film properties (transparency and UV-vis barrier), WVP, film water solubility at 25 °C (Solub 25 °C), film thickness, mechanical properties (EB, EM and TS), the ratios of the absorbances of FTIR peaks 1022/995 and 1045/1022, crystallinity degree (CD), percentage of biodegradation at 90 days (BD), Ag migration in acetic acid simulant (Ag/AA) and water (Ag/water) and characteristics of synthetized nanoparticles as the mean diameter and **ζ** of the filmogenic suspensions that contain them.

3.3. Cytotoxicity evaluation of nanocomposite films

The cytotoxicity assays allow the evaluation of the cellular response against a potentially toxic agent. Considering that the cytotoxic effects of AgNPs depend on the cell line used, three different cell types were tested. Caco-2/TC7 cell line (of human colon adenocarcinoma origin) is the most popular *in vitro* model for the toxicological evaluation of the nanomaterials due to the similar structure and function with the enterocytes (Tibolla et al., 2019). In addition, the TC7 clone has the advantage of differentiating in 7 days (Chantret et al, 1994). Vero cells are fibroblastic monkey cells and widely used as cytotoxic assay models due to their sensitivity to different treatments (Popoff, 1987) and THP-1 is a human leukemia monocytic cell line accepted as a good model for immunological studies (Assad et al., 2021a; Chanput et al., 2013; Z. Qin, 2012).

The mitochondrial activity of Vero and Caco-2/TC7 cells exposed to control (CM, CS and CL) and nanocomposite (AgNP L and AgNP *in situ*) films for 24 h are shown in Figure 4.a. The films with AgNPs *in situ* (143 ppm) were less cytotoxic for the Caco-2/TC7 line (90% viability) compared to CL and AgNP L films. The observed effect on human intestinal epithelial cells may be since the AgNPs, synthesized *in situ* in the filmogenic suspension and coated by the starch, are more integrated in the polymer matrix, less exposed and therefore their interaction with the cells is limited. Yu et al. (2019) studied the effect of different concentrations (50 - 1000 μg/ml) of AgNPs and cellulose nanofibers on the viability of Caco-2 cells and according with to the MTT assay, they observed no significant decrease in the number of viable cells until the added concentration was 1000 μg/ml. Considering the obtained results and the cytotoxicity classification based on the percentage of viability (100%–75%) established by the ISO 10993 standard (Young et al., 2005), the films with AgNPs *in situ* did not show any toxic effect on human colon cells after 24 h of contact.

For Vero cells significant differences ($p<0.05$) were observed between CM and all the samples tested, either nanocomposite films or their controls. This result may be related to the adhesion differences observed between the film and Vero cells, possibly due to the matrix formulation (starch and glycerol). These results support the use of different cell lines to evaluate cytotoxic effects.

Some factors such as shape, capping, zeta potential, and diameter can be critical for the toxicity of the AgNPs, especially for those with diameters ≤ 10 nm (Liao et al., 2019; Palem et al., 2018; Rolim et al., 2019; Yu et al., 2019). In this sense, no significant differences were observed between the films with AgNP L of 5.5 ± 0.8 nm diameter and their respective control for the cell lines studied. Although there is a decrease in cell viability, it is greater than 60% for both CL and AgNP L samples. This result can be related to the acidity of the materials to the cell medium, since the initial filmogenic suspension had an average pH of 3.0. However, the DMEM color did not change throughout the test indicating that the film did not affect the medium pH. Rolim et al. (2019) synthesized AgNPs using tea polyphenols and mentioned that, in addition to being capping agents, these compounds can act as antioxidant and anti-inflammatory agents, decreasing the nanoparticles' toxicity.

AgNP L was stabilized with citric and ascorbic acid, and other compounds such as polyphenols and flavonoids present in the lemon juice (Ortega et al., 2021), so a minor or reversible cell damage would be expected if the signal pathways activated are not necrotic. However, an effect on the viability of Caco-2/TC7 and Vero cells was observed, indicating the prevalence of other factors.

Considering these results and the cytotoxicity classification based on the percentage of viability (74%–50%) of the ISO 10993 norm (Young et al., 2005) the AgNP L films would be slightly cytotoxic.

Exposure to NPs and their subsequent uptake even affects phagocytic lines such as macrophages derived from THP-1 cells. Monocytic THP-1 cells exhibited reduced phagocytic capacity compared to macrophages, because the latter have surface markers that allow them to engulf bacteria or particles by phagocytosis compared to undifferentiated cells (Lunov et al., 2011). Figure 4b and c show the percentage of propidium iodide labeled dead cells (% of IP+ cells) for each film sample. Under the assay conditions, regardless of the sample analyzed, no significant differences ($p>0.05$) in necrotic monocytic THP-1 cells were observed (Fig. 4b). These cells are prepared to remove exogenous particles or bacteria, thus protecting against external attack. Furthermore, the assay was performed with 24 h incubation and maintained FBS content, which may interfere with the effect of NPs. It has been shown that there may be differences in nanoparticle capture in the presence and absence of FBS; however, Kettler et al. (2016) have suggested that the presence of serum is necessary to maintain cell viability.

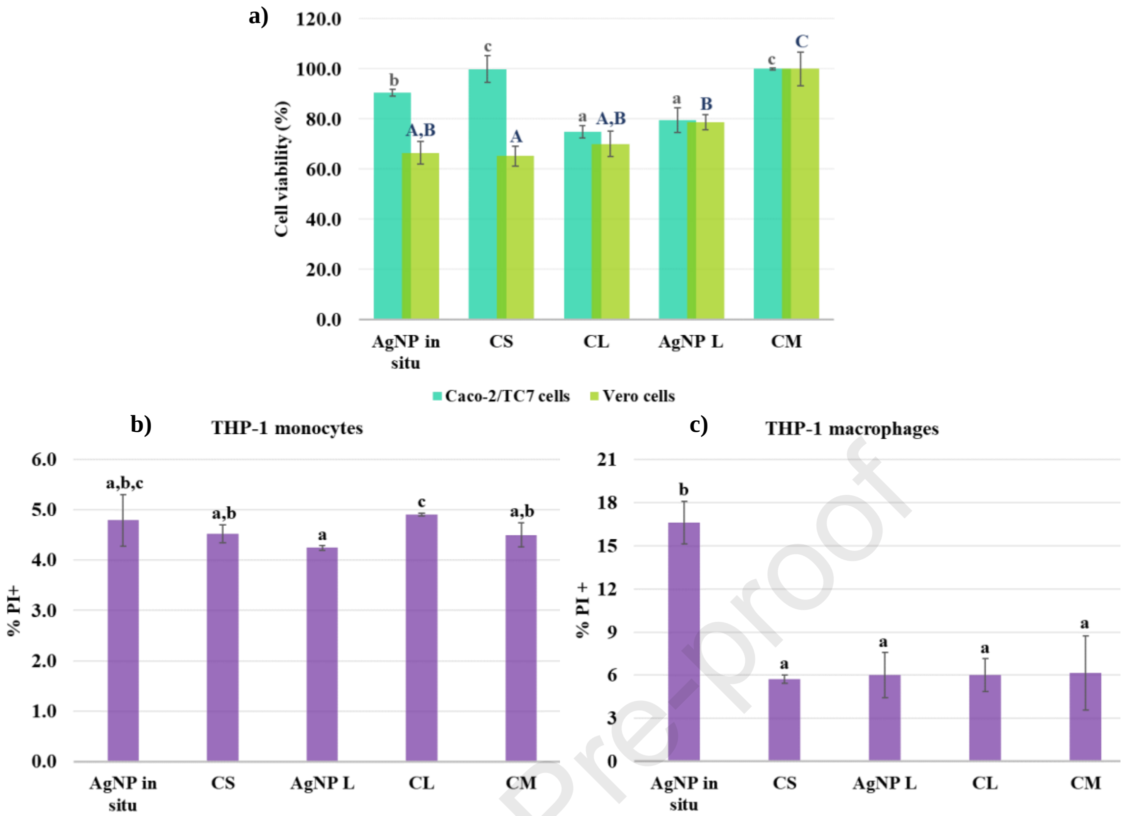

Figure 4: Cytotoxic effect of control and nanocomposite films on a) Caco-2/TC7 and Vero cells, b) THP-1 as monocytes and c) macrophages.

Figure 4.c showed that only AgNPs *in situ* films were significantly different ($p<0.05$) from the control for THP-1 cells differentiated to macrophages. This behavior may be due to the low concentration of AgNP L (71.5 ppm) included in the nanocomposite films, and because the nanoparticles are capped with the phytochemical components of lemon with proven anti-inflammatory action. Besides it is important to remark that the percentage of IP+ are within the range of DMEM control (Assad 2021 personal communication) consequence of experimental procedure, indicating the absence of cytotoxic effect.

The differences observed between monocyte and macrophage cells may be associated with the expression of different markers (Assad et al., 2021; Chanput et al., 2013). Lunov et al. (2011) reports that to the macrophages, in serum presence, the CD64 receptor participates in the uptake of foreign particles by phagocytosis. Thus, the response to an exogenous stimulus is different whether it is against differentiated or undifferentiated THP-1 cells, and especially when certain markers are studied (Assad et al., 2021).

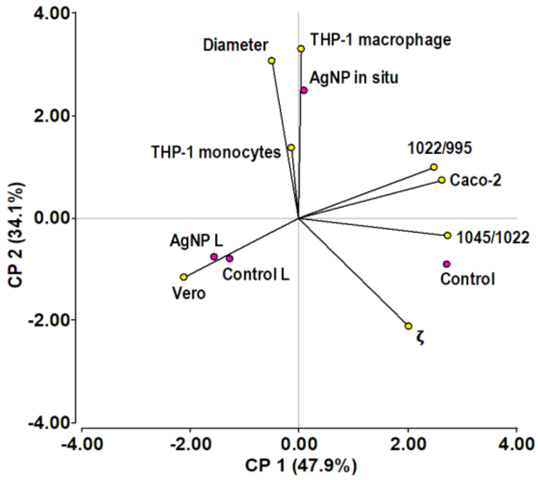

Figure 5: Biplot graph resulting from the PCA of the viability of the three cell lines tested and the characteristics of the nanocomposite materials (yellow dots) containing AgNP *in situ* and AgNP L (red dots). The parameters analyzed were the Caco-2/TC7 and Vero cells' viability and the % of THP-1 cells (monocytes and macrophages) positive for PI, the ratios of the FTIR peaks 1022/995 and 1045/1022, and characteristics of nanoparticles as the mean diameter and **ζ** of the suspensions that contain them.

The PCA including characteristics of AgNP *in situ* and AgNP L, and viability of Caco-2/TC7, Vero and % THP-1 cells (monocytes and macrophages) is shown in Figure 5. Two principal components explained 82% of the total variance. CP1 (with the 47.9%) discriminated between the materials with and without CA and CP2 (which described 34.1% of the total variance) was associated with the type of nanoparticles incorporated into the starch suspension.

The CP1 component correlates linearly with the Caco-2/TC7 cells viability and the absorbance ratio of the FTIR peaks (related to the amorphous-crystalline phase amount of the films). CP2 was associated with the viability of THP-1 monocytic cells and differentiated to macrophages and the nanoparticles' diameter. Both components allowed to explain the viability of Vero cells (CP1= -0.76 and CP2= -0.35) and the **ζ** (CP1= 0.73 and CP2= -0.64). The cophenetic correlation was 0.964, indicating that the grouping of variables performed was satisfactory.

3.4. Application of nanomaterials as food packaging on cheese

Finally, active packages were developed by thermo-sealing the nanocomposite and control films, as shown in Figure.6a, which were used to package soft cheese and were stored at 4 ºC for 21 days. The cheese shelf-life was defined as the time required to reach 10^6 CFU/g of sample (López et al., 2011) and was determined by counting molds and yeasts. The shelf-life of the cheese control sample was 14 days, while those packaged with the nanocomposite and CL films showed an average shelf-life of 21 days (Fig. 6b). Although the nanocomposite samples were able to extend the shelf-life, the CL and AgNP L films were more effective, probably because of the synergic effect of the compounds present in the lemon juice, such as flavonoids, polyphenols, organic acids, and the low pH of the film-forming suspension. Antifungal activity of citrus flavonoids has been widely investigated, as mentioned by Jing et al. (2014). Even though the antifungal effects of natural compounds can be affected by a wide variety of factors, some studies have shown that terpenes and phenolic compounds can damage the membrane of certain fungi and microorganisms denaturing proteins (Sikkema, de Bont, & Poolman, 1995).

AgNPs are well known for their antimicrobial properties against various pathogens, including bacteria and fungi, but the mechanisms responsible for this activity are not well established to date and are still a topic of debate. In fungi, the exposure to AgNPs causes cellular deformation through interaction with unsaturated fatty acids, which increases the permeability of the cell membrane, resulting in the loss of water, salts, proteins, and some intracellular components that affect the viability and budding process of fungal cells (Al-Otibi et al., 2022; Meneses et al., 2022). On the other hand, a strong reduction in mycelial growth was also observed by Al-Otibi et al. (2022), while Lee et al. (2019) detected an increase in reactive oxygen species (ROS) production after exposure to AgNPs in *C. albicans* but not in *Saccharomyces cerevisiae*. With respect to antimicrobial activity, several studies suggest that AgNPs are effective on both Gram-negative and Gram-positive strains. They cause cell damage and subsequent death through the generation of ROS, free radicals derived from the surface of AgNPs, silver ion stress, interactions with the bacterial cell that lead to depletion of intracellular ATP levels and damage to respiratory enzymes, among others. These mechanisms depend on the size, shape, charge, concentration, and capping agent of the nanoparticles (Liao et al., 2019; Vanlalveni et al., 2021).

For AgNP L and CL films, the count of lactic acid bacteria after 21 days of cheese storage, were similar at the initial content (7.15 ± 0.04 log CFU/g for AgNP L, 7.40 ± 0.40 log CFU/g for CL, being the initial count for both 7.09 ± 0.01 log CFU/g). Similar results were described by Incoronato et al. (2011), who observed that the incorporation of AgNPs did not affect the growth of functional lactic acid bacteria in samples of Fior di Latte cheese stored at 10 ºC.

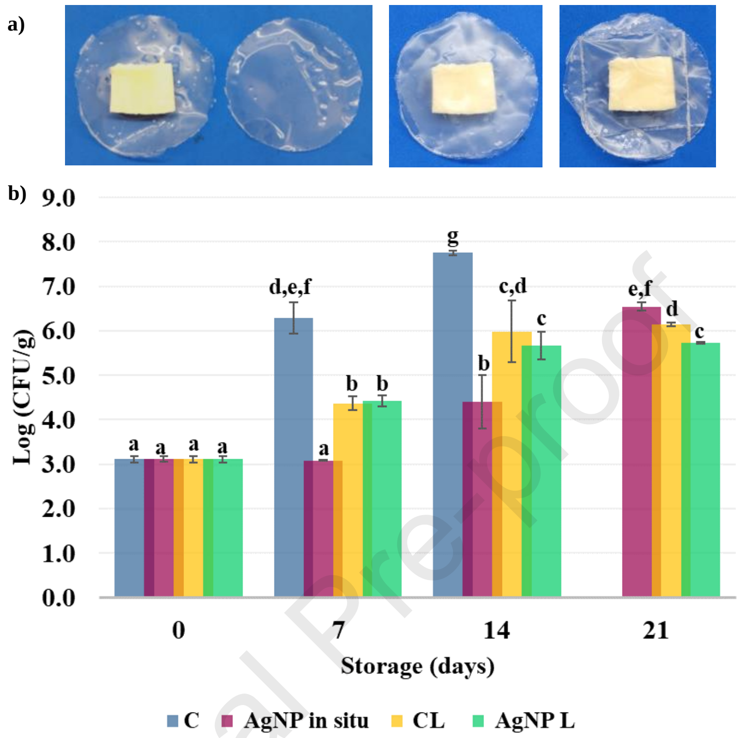

Figure 6: a) Cheese packages obtained by thermo-sealing of the films. b) Impact of different packaging on shelf-life of refrigerated cheese samples.

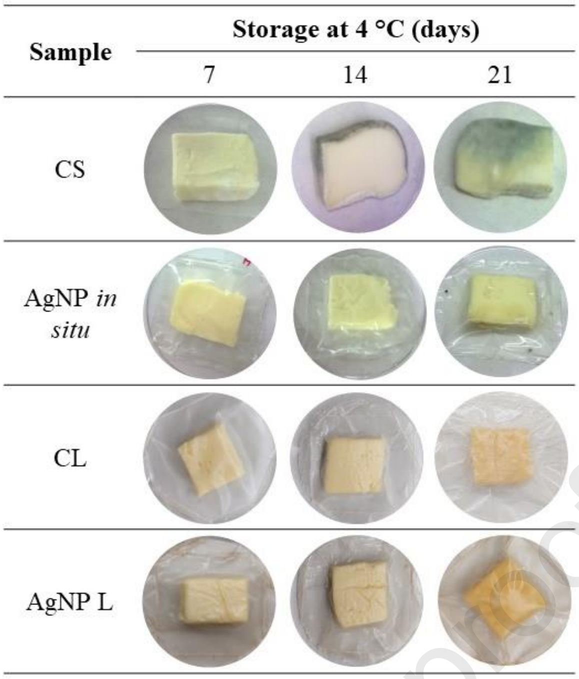

Figure 7: Photographs of cheese samples packaged with CS, AgNP *in situ*, CL, and AgNP L films, respectively, and stored at 4 °C.

Figure 7 shows the corresponding photographs of the packaged cheese samples after 7, 14, and 21 days of storage at 4 °C. Visually, the cheese samples packaged with films containing AgNPs *in situ* showed an absence of yeast and mold on the samples' surfaces after 14 days. This agrees with the results of the shelf-life previously mentioned. On the other hand, it was observed that after 21 days, CL and AgNP L films did not show any spoilage, although they evidence a slight increase in the coloration of the samples, probably due to the dehydration of the samples.

Consumer preference for natural foods has been a limiting factor for the implementation of nano-packaging technologies (Padmanabhan et al., 2018). However, an increase in the development of these technologies in conjunction with evidence on risk assessment could help to remove consumer concerns and enable further development of the active food packaging market. Production costs and the current legislative framework for this type of material were evaluated, and further progress is still needed in this regard.

Table 2 shows the production cost analysis of the nanocomposite films. For this purpose, the market prices of the components of the formulations were considered: corn starch, glycerol, $AgNO_3$, maltose, and lemon. To obtain the production cost for the formulations it was considered that to obtain 1 m^2 of film, 3140 g of filmogenic suspension were needed, since a constant molding ratio of 3.14 kg/m^2 was used. The costs associated with energy consumption, salaries, and the used equipment were not considered.

Table 2: Production cost analysis of nanocomposite films

Components price (u$s)	Suspension content required for 1m^2 film	Contribution to the cost (u$s)
	AgNPs *in situ* films	
Corn starch (1.50/Kg)	94.2000 g	0.14
Maltose (106/500 g)	0.8164 g	0.17
$AgNO_3$, ACS, 99,9+% (87.90/25 g)	0.7062 g	2.48
Glycerol, ACS, 99,9+% (111/L)	28.2600 g	2.48
Total cost for 1 m^2 of film		5.27
	AgNP L	
Lemon juice (0,24/100 ml)	80 ml	0.24
$AgNO_3$, ACS, 99,9+% (87.90/25g)	0.0221 g	0.08
Total cost for 100 ml of AgNP L		0.32
	AgNP L films	
Corn starch (1.50/Kg)	94.2000 g	0.14
AgNP L	60.4 ml	0.19
Glycerol, ACS, 99,9+% (111/L)	28.2600 g	2.48
Total cost for 1 m^2 of film		2.81

The reagents' costs were obtained from www.alfa.com, except for corn starch, which was taken from Mercado Libre Argentina (www.mercadolibre.com.ar) and lemon from www.alimentosargentinos.gob.ar.

In addition, it is important to point out that high-value by-products can be obtained from the peels, pulps, and seeds remaining after obtaining lemon juice, such as lemon essential oil and citrus-pectins, as well as concentrates, cremogenates, and other derivatives. Furthermore, citrus peel extracts can be used to obtain AgNPs (Kahrilas et al., 2014; Kaviya et al., 2011). Therefore, the use of by-products and waste contributes to the design of sustainable processes, considering the premises of the circular economy.

Likewise, the advantages of these nanocomposite films as food packaging compared to other food packaging materials are there: high bio-desintegration rate and antimicrobial capacity without conferring cytotoxic characteristics.

4. Conclusion

The synthesis of AgNPs using by-products and environmentally friendly reagents allows to obtain stable particles with variable size and morphology in a short time with simple techniques. Smaller and more stable AgNPs, than those synthesized *in situ*, were obtained by using lemon juice as a reducing, *capping* and stabilizing agent (AgNP L) without affecting the filmogenic capacity of the suspension.

While both nanocomposite materials exhibited desirable properties for food packaging, including antimicrobial capacity against food-borne pathogens, films with AgNP L showed better mechanical and barrier properties than those with AgNPs *in situ* and require low production costs. Lemon juice, in addition to providing compounds necessary for the nanoparticles' synthesis, contains components with crosslinking and/or plasticizing action of the polymeric matrix and others, such as polyphenols, that can protect cells from possible cytotoxic damage.

Likewise, considering the cytotoxicity classification based on the percentage of cell viability on Caco-2/TC7 and Vero cells as well as THP-1 cell line, nanocomposite materials containing both AgNP *in situ* and AgNP L are not potentially cytotoxic.

Active packaging obtained by heat-sealing the films extended the shelf- life of cheese by 7 days under refrigerated conditions, being those containing AgNP L. Finally, with a view to a future application, the current regulatory framework that considers this type of materials has been revised. Thus, considering the migration test previously performed, the developed nanocomposite films comply with the limits established by both EU legislation and MERCOSUR. Therefore, it is expected that a wide spectrum of possible applications will open for these materials.

Acknowledgements

The authors gratefully acknowledge the financial support provided by Agencia Nacional de Promoción Científica y Tecnológica de Argentina (PICT 2019-2827), CONICET and Universidad Nacional de La Plata (UNLP).

References

Abdallah, O. M., EL-Baghdady, K. Z., Khalil, M. M. H., El Borhamy, M. I., & Meligi, G. A. (2020). Antibacterial, antibiofilm and cytotoxic activities of biogenic polyvinyl alcohol-silver and chitosan-silver nanocomposites. *Journal of Polymer Research*, *27*(3), 1–9. https://doi.org/10.1007/s10965-020-02050-3

Al-Otibi, F., Alfuzan, S. A., Alharbi, R. I., Al-Askar, A. A., AL-Otaibi, R. M., al Subaie, H. F., & Moubayed, N. M. S. (2022). Comparative study of antifungal activity of two preparations of green silver nanoparticles from *Portulaca oleracea* extract. *Saudi Journal of Biological Sciences*, *29*(4), 2772–2781. https://doi.org/10.1016/j.sjbs.2021.12.056

Assad, S. E., Rolny, I. S., Minnaard, J., & Pérez, P. F. (2021). Bifidobacteria from human origin: interaction with phagocytic cells. *Journal of Applied Microbiology*, *130*(4), 1357–1367. https://doi.org/10.1111/jam.14861

Böhmert, L., Girod, M., Hansen, U., Maul, R., Knappe, P., Niemann, B., Weidner, S. M., Thünemann, A. F., & Lampen, A. (2014). Analytically monitored digestion of silver nanoparticles and their toxicity on human intestinal cells. *Nanotoxicology*, *8*(6), 631–642. https://doi.org/10.3109/17435390.2013.815284

Cerqueira, M. A., Sousa-Gallagher, M. J., Macedo, I., Rodriguez-Aguilera, R., Souza, B. W. S., Teixeira, J. A., & Vicente, A. A. (2010). Use of galactomannan edible coating application and storage temperature for prolonging shelf-life of "Regional" cheese. *Journal of Food Engineering*, *97*(1), 87–94. https://doi.org/10.1016/J.JFOODENG.2009.09.019

Chanput, W., Mes, J. J., Savelkoul, H. F. J., & Wichers, H. J. (2013). Characterization of polarized THP-1 macrophages and polarizing ability of LPS and food compounds. *Food and Function*, *4*(2), 266–276. https://doi.org/10.1039/c2fo30156c

Hasanin, M., Elbahnasawy, M. A., Shehabeldine, A. M., & Hashem, A. H. (2021). Ecofriendly preparation of silver nanoparticles-based nanocomposite stabilized by polysaccharides with antibacterial, antifungal and antiviral activities. *BioMetals*, *34*(6), 1313–1328. https://doi.org/10.1007/s10534-021-00344-7

Hashem, A. M., Abuzeid, H., Kaus, M., Indris, S., Ehrenberg, H., Mauger, A., & Julien, C. M. (2018). Green synthesis of nanosized manganese dioxide as positive electrode for lithium-ion batteries using lemon juice and citrus peel. *Electrochimica Acta*, *262*, 74–81. https://doi.org/10.1016/j.electacta.2018.01.024

Incoronato, A. L., Conte, A., Buonocore, G. G., & Del Nobile, M. A. (2011). Agar hydrogel with silver nanoparticles to prolong the shelf life of Fior di Latte cheese. *Journal of Dairy Science*, *94*(4), 1697–1704. https://doi.org/10.3168/jds.2010-3823

Jayachandran, A., Aswathy, T., & Nair, A. (2021). Green synthesis and characterization of zinc oxide nanoparticles using *Cayratia pedata* leaf extract. *Biochemistry and Biophysics Reports*, *26*.

Jafarzadeh, S., Salehabadi, A., Mohammadi Nafchi, A., Oladzadabbasabadi, N., & Jafari, S. M. (2021). Cheese packaging by edible coatings and biodegradable nanocomposites; improvement in shelf life, physicochemical and sensory properties. *Trends in Food Science and Technology*, *116*, 218–231. https://doi.org/10.1016/j.tifs.2021.07.021

Jing, L., Lei, Z., Li, L., Xie, R., Xi, W., Guan, Y., Sumner, L. W., & Zhou, Z. (2014). Antifungal activity of citrus essential oils. In *Journal of Agricultural and Food Chemistry* (Vol. 62, Issue 14, pp. 3011–3033). American Chemical Society.

https://doi.org/10.1021/jf5006148

Kahrilas, G. A., Wally, L. M., Fredrick, S. J., Hiskey, M., Prieto, A. L., & Owens, J. E. (2014). Microwave-assisted green synthesis of silver nanoparticles using orange peel extract. *ACS Sustainable Chemistry & Engineering*, *2*(3), 367–376. https://doi.org/10.1021/sc4003664

Kaviya, S., Santhanalakshmi, J., Viswanathan, B., Muthumary, J., & Srinivasan, K. (2011). Biosynthesis of silver nanoparticles using *Citrus sinensis* peel extract and its antibacterial activity. *Spectrochimica Acta - Part A: Molecular and Biomolecular Spectroscopy*, *79*(3), 594–598. https://doi.org/10.1016/j.saa.2011.03.040

Kettler, K., Giannakou, C., de Jong, W. H., Hendriks, A. J., & Krystek, P. (2016). Uptake of silver nanoparticles by monocytic THP-1 cells depends on particle size and presence of serum proteins. *Journal of Nanoparticle Research*, *18*(9), 286. https://doi.org/10.1007/s11051-016-3595-7

Kim, M. H., Kim, T. H., Ko, J. A., Ko, S., Oh, J. M., & Park, H. J. (2019). Kinetic and thermodynamic studies of silver migration from nanocomposites. *Journal of Food Engineering*, *243*(September 2018), 1–8. https://doi.org/10.1016/j.jfoodeng.2018.08.028

Kraśniewska, K., Galus, S., & Gniewosz, M. (2020). Biopolymers-based materials containing silver nanoparticles as active packaging for food applications–A review. In *International Journal of Molecular Sciences* 21(3). MDPI AG. https://doi.org/10.3390/ijms21030698

Lambré, C., Barat Baviera, J. M., Bolognesi, C., Chesson, A., Cocconcelli, P. S., Crebelli, R., Gott, D. M., Grob, K., Lampi, E., Mengelers, M., Mortensen, A., Steffensen, I. L., Tlustos, C., Van Loveren, H., Vernis, L., Zorn, H., Castle, L., Di Consiglio, E., Franz, R., Hellwin, N., Merkel, S., Milana, M. R., Barthélémy, E., & Rivière, G. (2021). Safety assessment of the substance silver nanoparticles for use in food contact materials. *EFSA Journal*, *19(8)*, e06790. https://doi.org/10.2903/j.efsa.2021.6790

Lee, B., Lee, M. J., Yun, S. J., Kim, K., Choi, I. H., & Park, S. (2019). Silver nanoparticles induce reactive oxygen species-mediated cell cycle delay and synergistic cytotoxicity with 3-bromopyruvate in *Candida albicans*, but not in *Saccharomyces cerevisiae*. *International Journal of Nanomedicine*, *14*, 4801–4816. https://doi.org/10.2147/IJN.S205736

Leites Luchese, C., Menegotto Frick, J., & Tessaro, C. I. (2021). Influence of the incorporation form of waste from the production of orange juice in the properties of cassava starch-based films. *Food Hydrocolloids*, *117*, 106730. https://doi.org/10.1016/j.foodhyd.2021.106730

Liao, C., Li, Y., & Tjong, S. C. (2019). Bactericidal and cytotoxic properties of silver nanoparticles. *International Journal of Molecular Sciences*, *20*(2). https://doi.org/10.3390/ijms20020449

López, O. V. (2011). *Desarrollo, caracterización y aplicación de envases biodegradables a partir de almidón*. Universidad Nacional de La Plata.

López, O. V, Giannuzzi, L., Zaritzky, N. E., & García, M. A. (2013). Potassium sorbate-controlled release from corn starch film. *Materials Science and Engineering C*, *33*(3), 1583–1591.

López, O. V., Lecot, C. J., Zaritzky, N. E., & García, M. A. (2011). Biodegradable packages development from starch-based heat sealable films. *Journal of Food Engineering*, *105*(2), 254–263. https://doi.org/10.1016/j.jfoodeng.2011.02.029

Lucera, A., Mastromatteo, M., Conte, A., Zambrini, A. v., Faccia, M., & del Nobile, M. A. (2014). Effect of active coating on microbiological and sensory properties of fresh mozzarella cheese. *Food Packaging and Shelf Life*, *1*(1), 25–29. https://doi.org/10.1016/J.FPSL.2013.10.002

Lunov, O., Syrovets, T., Loos, C., Beil, J., Delacher, M., Tron, K., Nienhaus, G. U., Musyanovych, A., Mailänder, V., Landfester, K., & Simmet, T. (2011). Differential uptake of functionalized polystyrene nanoparticles by human macrophages and a monocytic cell line. *ACS Nano*, *5*(3), 1657–1669. https://doi.org/10.1021/nn2000756

Mangaraj, S., Yadav, A., Bal, L. M., Dash, S. K., & Mahanti, N. K. (2019). Application of biodegradable polymers in food packaging industry: a comprehensive review. *Journal of Packaging Technology and Research*, *3*(1), 77–96. https://doi.org/10.1007/s41783-018-0049-y

Mathew, S., Jayakumar, A., Kumar, V. P., Mathew, J., & Radhakrishnan, E. K. (2019). One-step synthesis of eco-friendly boiled rice starch blended polyvinyl alcohol bionanocomposite films decorated with *in situ* generated silver nanoparticles for food packaging purpose. *International Journal of Biological Macromolecules*, *139*, 475–485. https://doi.org/10.1016/j.ijbiomac.2019.07.187

Meneses, M. L., Recalde, M., Martin, P. L., & Pardo, A. G. (2022). Antifungal activity of silver nanoparticles and clotrimazole against *Candida spp*. *Brazilian Journal of Pharmaceutical Sciences*, *58*. https://doi.org/10.1590/s2175-97902022e18719

Minnaard, J., Humen, M., & Pérez, P. F. (2001). Effect of *Bacillus cereus* exocellular factors on human intestinal epithelial cells. *Journal of Food Protection*, *64*(10), 1535–1541. https://doi.org/10.4315/0362-028X-64.10.1535

Mohan, S., Oluwafemi, O. S., Songca, S. P., Jayachandran, V. P., Rouxel, D., Joubert, O., Kalarikkal, N., & Thomas, S. (2016). Synthesis, antibacterial, cytotoxicity and sensing properties of starch-capped silver nanoparticles. *Journal of Molecular Liquids*, *213*, 75–81. https://doi.org/10.1016/j.molliq.2015.11.010

Noshirvani, N., Ghanbarzadeh, B., Rezaei Mokarram, R., & Hashemi, M. (2017). Novel active packaging based on carboxymethyl cellulose-chitosan-ZnO NPs nanocomposite for increasing the shelf life of bread. *Food Packaging and Shelf Life*, *11*, 106–114. https://doi.org/10.1016/j.fpsl.2017.01.010

Ortega, F., Arce, V. B., & Garcia, M. A. (2021). Nanocomposite starch-based films containing silver nanoparticles synthesized with lemon juice as reducing and stabilizing agent. *Carbohydrate Polymers*, *252*. https://doi.org/10.1016/j.carbpol.2020.117208

Ortega, F., García, M. A., & Arce, V. B. (2019). Nanocomposite films with silver nanoparticles synthesized *in situ*: Effect of corn starch content. *Food Hydrocolloids*, *97*. https://doi.org/10.1016/j.foodhyd.2019.105200

Ortega, F., Giannuzzi, L., Arce, V. B., & García, M. A. (2017). Active composite starch films containing green synthetized silver nanoparticles. *Food Hydrocolloids*, *70*, 152–162. https://doi.org/10.1016/j.foodhyd.2017.03.036

Ortega, F., Sobral, P., Jios, J. L., Arce, V. B., & García, M. A. (2022). Starch nanocomposite films: Migration studies of nanoparticles to food simulants and bio-disintegration in Soil. *Polymers*, *14*(9). https://doi.org/10.3390/polym14091636

Padmanabhan, S. C., Cruz-Romero, M. C., Kerry, J. P., & Morris, M. A. (2018). Food packaging: Surface engineering and commercialization. In *Nanomaterials for Food Packaging: Materials, Processing Technologies, and Safety Issues*. Elsevier Inc. https://doi.org/10.1016/B978-0-323-51271-8.00011-5

Palem, R. R., Ganesh, S. D., Kronekova, Z., Sláviková, M., Saha, N., & Saha, P. (2018). Green synthesis of silver nanoparticles and biopolymer nanocomposites: A comparative study on physico-chemical, antimicrobial and anticancer activity. *Bulletin of Materials Science*, *41*(2). https://doi.org/10.1007/s12034-018-1567-5

Polat, S., Fenercioğlu, H., & Güçlü, M. (2018). Effects of metal nanoparticles on the physical and migration properties of low-density polyethylene films. *Journal of Food Engineering*, *229*, 32–42. https://doi.org/10.1016/j.jfoodeng.2017.12.004

Popoff, M. R. (1987). Purification and characterization of *Clostridium sordellii* lethal toxin and cross-reactivity with *Clostridium difficile* cytotoxin. *Infection and Immunity*, *55*(1), 35–

43. https://doi.org/10.1128/iai.55.1.35-43.1987

Qin, Y., Liu, Y., Yuan, L., Yong, H., & Liu, J. (2019). Preparation and characterization of antioxidant, antimicrobial and pH-sensitive films based on chitosan, silver nanoparticles and purple corn extract. *Food Hydrocolloids*, *96*, 102–111. https://doi.org/10.1016/j.foodhyd.2019.05.017

Qin, Z. (2012). The use of THP-1 cells as a model for mimicking the function and regulation of monocytes and macrophages in the vasculature. In *Atherosclerosis* (Vol. 221, Issue 1, pp. 2–11). https://doi.org/10.1016/j.atherosclerosis.2011.09.003

Rafique, M., Sadaf, I., Rafique, M. S., & Tahir, M. B. (2017). A review on green synthesis of silver nanoparticles and their applications. *Artificial Cells, Nanomedicine and Biotechnology*, *45*(7), 1272–1291. https://doi.org/10.1080/21691401.2016.1241792

Rather, R. A., Sarwara, R. K., Das, N., & Pal, B. (2018). Impact of reducing and capping agents on carbohydrates for the growth of Ag and Cu nanostructures and their antibacterial activities. *Particuology*, 1–8. https://doi.org/10.1016/j.partic.2018.01.004

Reddy, N., & Yang, Y. (2010). Citric acid cross-linking of starch films. *Food Chemistry*, *118*(3), 702–711. https://doi.org/10.1016/j.foodchem.2009.05.050

Rizzotto, F., Vasiljevic, Z. Z., Stanojevic, G., Dojcinovic, M. P., Jankovic-Castvan, I., Vujancevic, J. D., Tadic, N. B., Brankovic, G. O., Magniez, A., Vidic, J., & Nikolic, M. V. (2022). Antioxidant and cell-friendly Fe_2TiO_5 nanoparticles for food packaging application. *Food Chemistry*, *390*. https://doi.org/10.1016/j.foodchem.2022.133198

Rolim, W. R., Pelegrino, M. T., de Araújo Lima, B., Ferraz, L. S., Costa, F. N., Bernardes, J. S., Rodigues, T., Brocchi, M., & Seabra, A. B. (2019). Green tea extract mediated biogenic synthesis of silver nanoparticles: Characterization, cytotoxicity evaluation and antibacterial activity. *Applied Surface Science*, *463*, 66–74. https://doi.org/10.1016/J.APSUSC.2018.08.203

Sarwar, N., Humayoun, U. Bin, Kumar, M., Zaidi, S. F. A., Yoo, J. H., Ali, N., Jeong, D. I., Lee, J. H., & Yoon, D. H. (2021). Citric acid mediated green synthesis of copper nanoparticles using cinnamon bark extract and its multifaceted applications. *Journal of Cleaner Production*, *292*, 125974. https://doi.org/10.1016/j.jclepro.2021.125974

Selvakumar, P. M., Antonyraj, C. A., Babu, R., Dakhsinamurthy, A., Manikandan, N., & Palanivel, A. (2016). Green synthesis and antimicrobial activity of monodispersed silver nanoparticles synthesized using lemon extract. *Synthesis and Reactivity in Inorganic, Metal-Organic, and Nano-Metal Chemistry*, *46*(2), 291–294. https://doi.org/10.1080/15533174.2014.971810

Shi, R., Bi, J., Zhang, Z., Zhu, A., Chen, D., Zhou, X., Zhang, L., & Tian, W. (2008). The effect of citric acid on the structural properties and cytotoxicity of the polyvinyl alcohol/starch films when molding at high temperature. *Carbohydrate Polymers*, *74*(4), 763–770. https://doi.org/10.1016/j.carbpol.2008.04.045

Sikkema, J., De Bont, J. A. M., & Poolman, B. (1995). Mechanisms of membrane toxicity of hydrocarbons. *Microbiological Reviews*, *59*(2), 201–222. https://doi.org/10.1128/mmbr.59.2.201-222.1995

Störmer, A., Bott, J., Kemmer, D., & Franz, R. (2017). Critical review of the migration potential of nanoparticles in food contact plastics. *Trends in Food Science and Technology*, *63*, 39–50. https://doi.org/10.1016/j.tifs.2017.01.011

Tibolla, H., Pelissari, F. M., Martins, J. T., Lanzoni, E. M., Vicente, A. A., Menegalli, F. C., & Cunha, R. L. (2019). Banana starch nanocomposite with cellulose nanofibers isolated from banana peel by enzymatic treatment: *In vitro* cytotoxicity assessment. *Carbohydrate Polymers*, *207*(May 2018), 169–179. https://doi.org/10.1016/j.carbpol.2018.11.079

Vanlalveni, C., Lallianrawna, S., Biswas, A., Selvaraj, M., Changmai, B., & Rokhum, S. L. (2021). Green synthesis of silver nanoparticles using plant extracts and their antimicrobial activities: a review of recent literature. In *RSC Advances* (Vol. 11, Issue 5, pp. 2804–2837). Royal Society of Chemistry. https://doi.org/10.1039/d0ra09941d

Versino, F., & García, M. A. (2019). Particle size distribution effect on cassava starch and cassava bagasse biocomposites. *ACS Sustainable Chemistry and Engineering*, *7*(1), 1052–1060. https://doi.org/10.1021/acssuschemeng.8b04700

Young, F. M., Phungtamdet, W., & Sanderson, B. J. S. (2005). Modification of MTT assay conditions to examine the cytotoxic effects of amitraz on the human lymphoblastoid cell line, WIL2NS. *Toxicology in Vitro*, *19*(8), 1051–1059. https://doi.org/10.1016/j.tiv.2005.05.001

Yu, Z., Wang, W., Kong, F., Lin, M., & Mustapha, A. (2019). Cellulose nanofibril/silver nanoparticle composite as an active food packaging system and its toxicity to human colon cells. *International Journal of Biological Macromolecules*, *129*, 887–894. https://doi.org/10.1016/j.ijbiomac.2019.02.084

Zhai, X., Li, Z., Zhang, J., Shi, J., Zou, X., Huang, X., Zhang, D., Sun, Y., Yang, Z., Holmes, M., Gong, Y., & Povey, M. (2018). Natural biomaterial-based edible and pH-sensitive films combined with electrochemical writing for intelligent food packaging. *Journal of Agricultural and Food Chemistry*, *66*(48), 12836–12846. https://doi.org/10.1021/acs.jafc.8b04932

Silver nanoparticles were synthesized by using two different green methods.

Nanocomposite starch-based films were developed and characterized.

Cytotoxicity of nanocomposite films was evaluated on three cell lines.

Nanocomposite packages were obtained by thermo-sealing.

Active packages extend the cheese shelf life under refrigerated conditions.

Author Statement

F. Ortega Conceptualization, Data curation; Formal analysis; Investigation; Methodology, Software; Writing original draft.

J. Minnaard: Conceptualization, Data curation; Formal analysis; Investigation; Methodology, Software; Writing review & editing, Supervision; Validation.

V.B. Arce: Investigation; Methodology, Supervision, Visualization

M.A. García: Conceptualization, Data curation, Supervision; Validation, Writing - review & editing

Funding acquisition; Investigation; Methodology; Project administration; Resources

Conflict of interest

Authors declare no conflict of interest